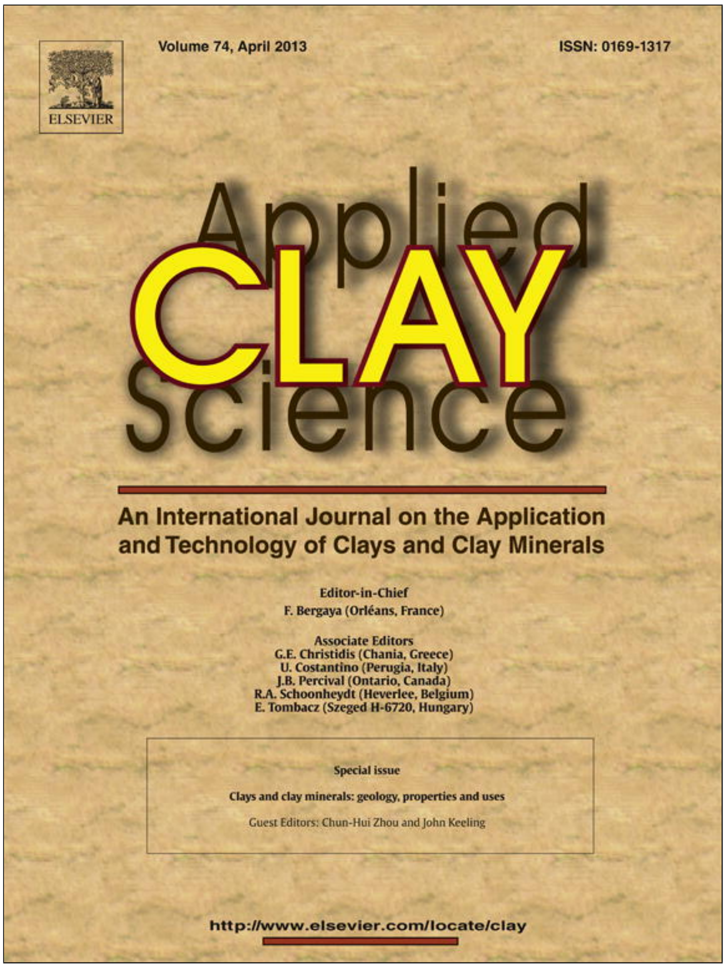
Volume 74, April 2013
ISSN: 0169-1317
ELSEVIER
Applied CLAY Science
An International Journal on the Application and Technology of Clays and Clay Minerals
Editor-in-Chief
F. Bergaya (Orléans, France)
Associate Editors
G.E. Christidis (Chania, Greece)
U. Costantino (Perugia, Italy)
J.B. Percival (Ontario, Canada)
R.A. Schoonheydt (Heverlee, Belgium)
E. Tombacz (Szeged H-6720, Hungary)
Special issue
Clays and clay minerals: geology, properties and uses
Guest Editors: Chun-Hui Zhou and John Keeling
http://www.elsevier.com/locate/clay

Applied Clay Science 74 (2013) 28–36

Contents lists available at SciVerse ScienceDirect

Applied Clay Science

journal homepage: www.elsevier.com/locate/clay

Research paper

Clay mineralogy indicates the Holocene monsoon climate in the Changjiang (Yangtze River) Catchment, China

Quan Wang, Shouye Yang *

State Key Laboratory of Marine Geology, Tongji University, Shanghai 200092, PR China

ARTICLE INFO

Article history:
Received 29 March 2012
Received in revised form 25 August 2012
Accepted 31 August 2012
Available online 9 October 2012

Keywords:
Clay mineralogy
Holocene
Monsoon climate
Changjiang River
Delta

ABSTRACT

The sediments from two cores (CM97 and LGZ) in the Changjiang (Yangtze River) Delta were collected for clay mineral analyses, with the aims of examining the origin of the clay and the application of clay mineralogy to the reconstruction of monsoon climate variability during the Holocene. The clay mineral assemblages of the Holocene sediments are similar overall to clays deposited in the modern Changjiang, albeit with large fluctuations in depositional environments. Peak contents of smectite occurring at ca. 13–11.5 ka are primarily due to the significant contribution of clays weathered from the upper Changjiang catchment under the impact of an enhanced Indian Summer Monsoon. The regular variations of crystallographic indices including illite crystallinity, chlorite crystallinity and chemical index of illite in the cores show close correspondence with the well-known oxygen isotopic curves of stalagmites in China. This suggests that the evolution of the Asian Summer Monsoon in the Changjiang catchment can be reliably reconstructed from variation in the weathering characteristics of the detrital clay component of sediments, despite the complex sediment source-to-sink transport patterns and the changes of depositional environments. For short timescales, the degree of crystallinity of clay minerals is more sensitive to chemical weathering and climate change than their absolute abundance. This study sheds new light on the reconstruction of paleoclimatic change in large drainage basins through the clayey sediments accumulated in estuarine and deltaic areas where land and sea interact.

1. Introduction

Although weaker in amplitude than the large climate fluctuation during the last glacial cycle, the variability of climate during the Holocene is considered to be larger and more frequent than previously recognized (Alley and Ágústsdóttir, 2005; An et al., 2000; Bond et al., 2001; Denton and Karlén, 1973; Dykoski et al., 2005; Fleitmann et al., 2007; Hong et al., 2005; Kleinen et al., 2011; Mayewski et al., 2004; Wang et al., 2005). Changes in solar insolation linked to Earth's orbital variations and solar intensity variability primarily account for global climate change during the Holocene (Dykoski et al., 2005; Hong et al., 2005; Mayewski et al., 2004; Wang et al., 2005). Climate change significantly affects biospheric evolution and human civilization in the Holocene (Chen et al., 2005b, 2008; deMenocal et al., 2000; Hodell et al., 1991), and thus, has attracted increasing research attention in recent decades.

Meanwhile, various archives, such as stalagmite (Dong et al., 2010; Dykoski et al., 2005; Hong et al., 2005; Wang et al., 2005), lacustrine and estuarine sediments (Chen et al., 2005a; Shi et al., 1993; Xiao et al., 2006; Zhang et al., 2011; Zong et al., 2006), palynological data (Atahan et al., 2008; Li et al., 2010; Liu et al., 1992, 1998; Shen et al., 2006; Yi and Saito, 2004; Yi et al., 2003a,b, 2006), ice core (Shi et al., 1999; Thompson et al., 2006), and ancient literatures (Chu, 1973; Zhang, 2006), have been used to reconstruct the Holocene climate in China, with emphasis on the spatial and temporal variability of the East Asian Summer Monsoon (EASM). In Liu et al. (1992, 1998), high abundance of pollen and spore between 10,000 and 4800 years B.P. suggests that the EASM during the early-mid Holocene probably extended beyond its present boundary to reach western Tibet in response to orbital forcing. An et al. (2000) suggested that peak precipitation of the EASM in the Holocene was asynchronous in central and eastern China, reaching the maximum at different times in different regions. In Wang et al. (2005) and Dykoski et al. (2005), the EASM intensity broadly follows the summer insolation. Zong et al. (2006) suggested that organic carbon compositions and diatom abundances in the Holocene sediments of the Zhujiang (Pearl River) Estuary can indicate the evolution of the EASM.

The Changjiang (Yangtze River) as the largest river originating from the eastern Tibetan Plateau, delivers a huge amount of terrigenous sediment from its vast catchment into the East China Sea, and has developed a large delta in the river mouth and unique

* Corresponding author at: State Key Laboratory of Marine Geology, Tongji University, 1239 Siping Road, Shanghai 200092, PR China. Tel.: +86 21 6598 9130; fax: +86 21 6598 6278.

E-mail address: syyang@tongji.edu.cn (S. Yang).

0169-1317/$ – see front matter © 2012 Elsevier B.V. All rights reserved.
http://dx.doi.org/10.1016/j.clay.2012.08.011

sedimentary systems on the shelf. The sediment that rapidly accumulated in the delta area during the Holocene is up to about 70 m in thickness (Hori et al., 2001a,b; Li et al., 2000), which makes the delta a natural laboratory for the study of land–sea interaction and paleoenvironmental change. Although the Holocene climate in China has been extensively studied as introduced above, only a few studies have paid special attention to the Changjiang catchment and delta area. This is mostly because of the lack of high quality research materials, reliable proxies, good age control of sedimentary strata and few high-resolution sampling analyses. In particular, sedimentary environments in the delta and estuary are more dynamic and interactive than those in the inland region and open ocean, and strong land–sea interaction results in frequent occurrence of hiatus. Previous research on the deltaic sediments used either a palynological approach or organic geochemical proxies to reconstruct the Holocene climate in the Changjiang catchment (Atahan et al., 2008; Chen et al., 2009; Liu et al., 1992, 1998; Yang et al., 2011; Yasuda et al., 2004; Yi and Saito, 2004; Yi et al., 2003a,b, 2006). From these studies, the drill core CM97 from Chongming Island in the Changjiang river mouth (Fig. 1) is now regarded as a classical borehole, and has been widely investigated in terms of its sediment stratigraphy and depositional facies (Hori et al., 2001a,b, 2002a,b), and environmental changes (Yang et al., 2011; Yi and Saito, 2004; Yi et al., 2003a,b, 2006). The core sediments are dated back to about 13 ka and allow us to plot the climate evolution through the Holocene in the Changjiang catchment.

In this paper, clay mineral assemblages of the sediments from Core CM97 were investigated and the proxies of clay mineral crystallinity were applied to link the weathering process, sediment transport and Holocene monsoon climate in the Changjiang drainage basin.

2. River setting

The Changjiang River originates from the northeast of the Tibet Plateau with an elevation of 6621 m and a drainage area of about 1.8×10^6 km^2, and flows about 6390 km eastward to the East China Sea (Fig. 1). The river delivers about 390×10^6 ton/year of suspended sediment and 896.4×10^9 m^3/year of water into the estuary based on the hydrological observation from 1950 to 2010 at Datong Gauge Station (China Ministry of Water Resources, 2011).

Geologically, the Changjiang catchment is primarily situated on the Yangtze Craton, and the upper basin was greatly affected by uplift of the Tibet Plateau during the Cenozoic, and the mid-lower basin was mostly shaped by the Paleozoic and Mesozoic tectonic movements. Diverse source rock types characterize the Changjiang catchment, which predominantly comprise Archean metamorphic rocks, Paleozoic carbonate and siliciclastic rocks, Mesozoic and Cenozoic igneous and clastic rocks, and Quaternary detrital sediments.

The Changjiang catchment is strongly influenced by a subtropical monsoon climate, which causes large seasonal and spatial variability in temperature, precipitation, runoff and fluvial discharge. The EASM played a key role in the climate evolution of the Changjiang basin during the Holocene, while the upper catchment may have been affected by the Indian Summer Monsoon (An et al., 2000; Dykoski et al., 2005; Mao et al., 2010).

3. Sample sources and analytic methods

Two cores were collected from the Changjiang Delta for the study of clay mineralogy. Core CM97 was drilled on Chongming Island in

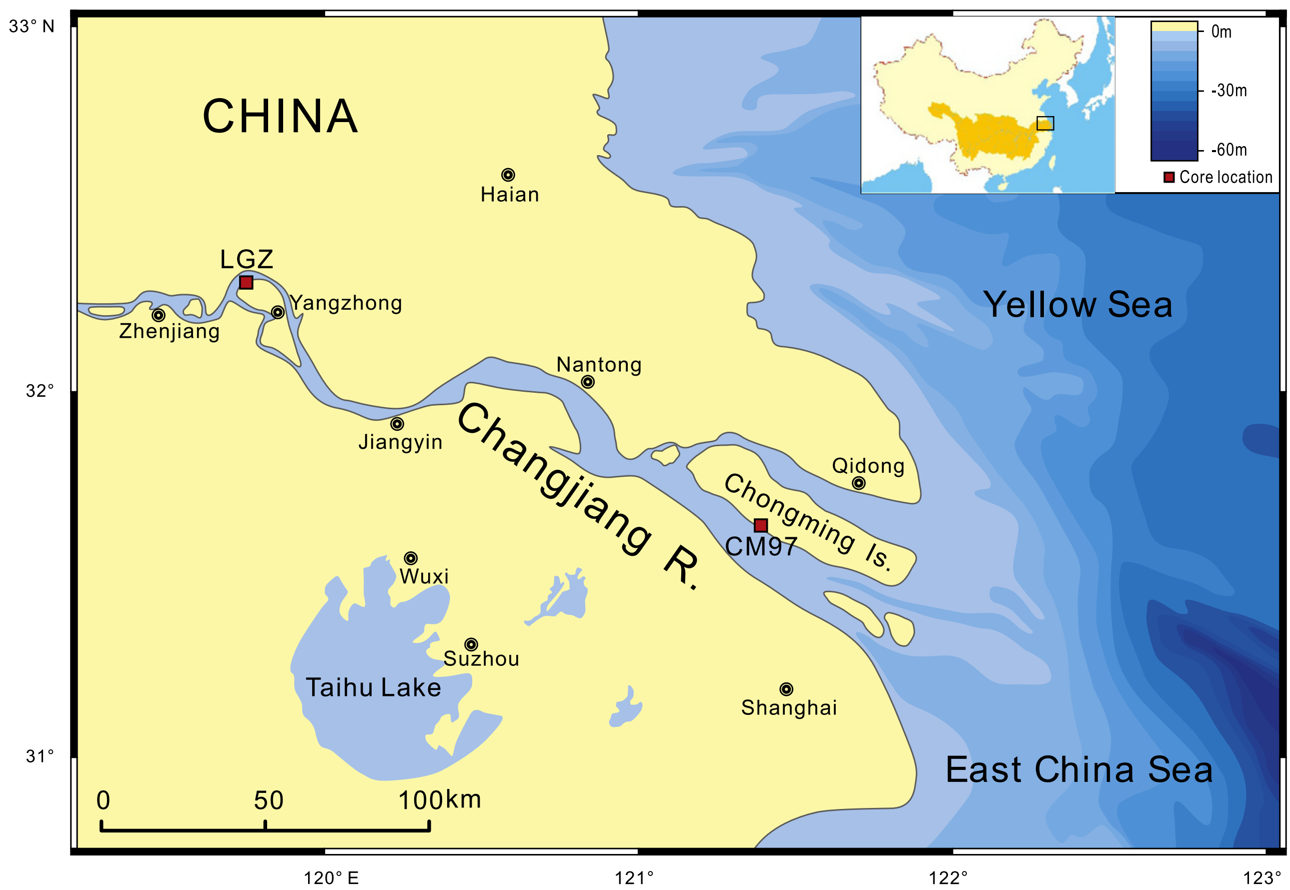

Fig. 1. A schematic map of the Changjiang Delta with the locations of Core CM97 and Core LGZ.

the present river mouth and the core length is 70.0 m. A short core, LGZ, of 2.0 m length was taken in a newly-formed bar in the lower Changjiang mainstream, about 150 km upstream from the river mouth (Fig. 1). Core LGZ is composed predominantly of clayey silt which accumulated over the last 150 years in the lower Changjiang mainstream, based on the ^{210}Pb geochronology (Zhan et al., 2010).

The sedimentary sequences of Core CM97 primarily consist of fluvial or river channel facies at the base (70.0–60.3 m in burial depth), with floodplain facies (60.3–43.2 m), estuarine facies (43.2–30.0 m), neritic facies (30.0–20.1 m) and deltaic facies at the top (20.1–0.0 m) (Fig. 2). Detailed sediment stratigraphy, delta evolution and sedimentary environment changes in the Changjiang delta and estuarine area during the postglacial period have been reported previously (Chen et al., 2005a; Hori et al., 2001a,b, 2002a,b; Li et al., 2000; Yi et al., 2003b, 2006). The dating of Core CM97 was based on ^{14}C from molluscan and snail shells (conventional ages, Hori et al., 2001b) and the radiocarbon ages used in this study refer to calendar years before present (BP, before 1950, Yi et al., 2003b, 2006).

Sediment grain size analysis was performed on 85 samples from Core CM97 using the laser grain size analyzer (Coulter LS230) at the State Key Laboratory of Marine Geology at Tongji University, after treating the samples with 10% H_2O_2 and 1 N HCl to respectively remove organic matter and carbonates. Results were reported in base 2 logarithmic phi (Φ) scale where $\Phi = -\log_2 D$ and D denotes diameter. For clay mineral analysis, 139 samples, including 119 from CM97 and 20 from LGZ, were measured by X-ray diffraction (XRD) on oriented clay fractions. Particles smaller than 2 μm were separated from the bulk sediment by the pipette method following the Stoke's Law, concentrated by centrifuging and then smeared on two glass slides. Three XRD measurements were carried out on each sample following the processes of air drying, ethylene–glycol saturated for 12 h, and heating at 500 °C for 2 h (Dou et al., 2010; Liu et al., 2003). The bulk samples were dispersed with longer whisking time instead of treating by 0.2 N HCl, in order to protect the very fine clay particles. X-ray diffractograms were obtained using a Rigaku D/max 2500 PC X-ray diffractometer in the Institute of First Oceanography in Qingdao, State Oceanic Administration. CuKα radiation and Ni filter were used, operated at 40 kV and 100 mA. Data were recorded from 3° to about 32° 2θ with a speed of 3°/min (2θ). The peak area percentages of major clay minerals were calculated from the XRD curve of the glycolated samples after manual baseline correction using Jade software version 5.0, following the semi-quantitative method of Biscaye (1965).

The illite crystallinity (IC), chlorite crystallinity (ChC) and chemical index of illite (CII) were calculated from the XRD diffractograms. The IC value was determined by measuring the full width at half maximum height of the 10 Å peak, and is expressed in °Δ2θ (Ji and Browne, 2000; Mao et al., 2010; Pandarinath, 2009; Pandarinath et al., 1999). Similarly, the ChC was measured on the 7 Å peak (Árkai and Ghabrial, 1997; Árkai et al., 1995; Mas et al., 2006) and also expressed in °Δ2θ. The CII refers to the ratio of the 5 Å and 10 Å peak areas. Ratios for the CII <0.5 may represent Fe–Mg-rich illite, while ratios >0.5 are primarily found in Al-rich illite (Mao et al., 2010).

4. Results

The sediment grain size and clay mineralogical composition of Core CM97 are shown in Fig. 2. The mean grain size (Mz) varied between 2.1 Φ and 7.3 Φ and exhibited irregular downcore variation. The bottom fluvial facies consisted of the coarsest sandy sediments with minor gravels, with a mean size of 4.5 Φ. The mean grain size gradually became finer from the fluvial facies upward to the neritic facies and the finest sediments were about 7.0 Φ in Mz. The deltaic facies at the top, however, became coarser and the average Mz was about 5.1 Φ. As shown in previous studies on clay mineralogy of the Changjiang-derived sediments (Dou et al., 2010; Fan et al., 2001; Gao et al., 2004; Mao et al., 2010; Wu et al., 2011; Yang et al., 2003), the clay minerals of Cores CM97 and LGZ sediments were dominated by illite, ranging from 19.8% to 68.7% and averaging at 56.7%. Kaolinite and chlorite yielded similar contents in the core sediments, with averages of 18.4±2.9% and 15.2±3.0% respectively. In comparison, smectite was less abundant but exhibited the largest downcore variation (2.1–70.0%) in Core CM97, and especially, reached the highest average content of 28.6% in the fluvial facies (Fig. 2).

In Core CM97, the illite crystallinity (IC) varied between 0.26 and 0.51 (°Δ2θ) and chlorite crystallinity (ChC) between 0.29 and 0.58 (°Δ2θ), while the chemical index of illite (CII) ranged from 0.32 to

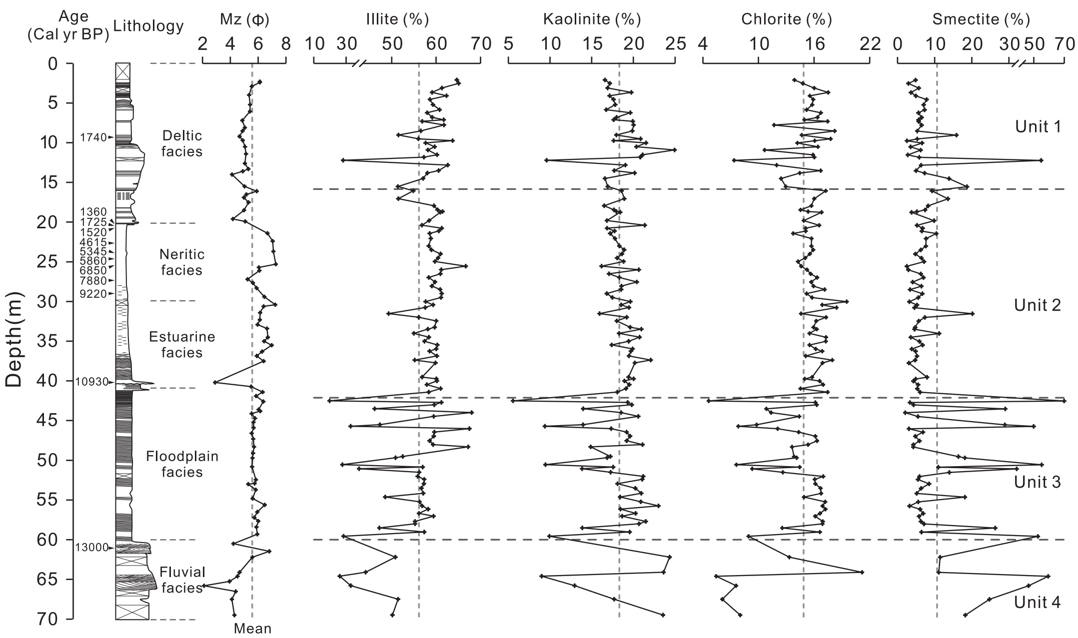

Fig. 2. Lithology of Core CM97 and depth profiles of mean grain size (Mz) and clay mineral contents. The lithology was modified from Hori et al. (2001b) and the age model (in calendar years before present) from Yi et al. (2003b).

1.04. Based on the downcore variations of clay mineral content and crystallinity index, Core CM97 was subdivided into four units: Unit 1 (0–16 m), Unit 2 (16–42 m), Unit 3 (42–60 m) and Unit 4 (60–70 m) (Fig. 3). The indices of IC, ChC and CII showed large but overall similar downcore fluctuations, with higher values in Unit 2 and lower in Unit 4. Remarkably, increasing trends of IC, ChC and CII values were clearly observed from Unit 4 to the lower part of Unit 3 and also from the upper Unit 3 to the middle part of Unit 2, whereas the obvious decrease of these indices occurred at the transition from Unit 2 to Unit 1.

5. Discussion

5.1. Provenance of clay minerals in the Changjiang Delta during the Holocene

Clay mineral assemblages in coastal and marine sediments are predominantly determined by sources of clayey sediment, provenance weathering, sediment transport and depositional processes (Chamley, 1989; Gao et al., 2004; Pandarinath, 2009; Pandarinath et al., 1999). Estuarine and delta areas of large rivers receive huge detrital loads from their vast drainage basins that can encompass a variety of geological, geographical and climatic environments. Consequently, the clayey sediments accumulated in the estuarine and delta areas typically represent an average composition of clay minerals sourced from the whole catchment (Singer, 1980, 1984).

The clay mineral assemblages of Cores CM97 and LGZ are overall similar to Changjiang-derived clays reported in previous studies (Fig. 4) (Dou et al., 2010; Fan et al., 2001; Fang et al., 2007; Gao et al., 2004; Mao et al., 2010; Wu et al., 2011; Yang, 1988; Yang et al., 2003). In the ternary diagram of (illite + smectite)–chlorite–kaolinite (Fig. 4), most of the samples in Core CM97 plot in the compositional range of Core LGZ (dashed circle) albeit with relatively scattered distribution. The sediments in Core LGZ that were deposited in the lower Changjiang mainstream over the last 150 years (Zhan et al., 2010), are definitely derived from the large drainage basin. Therefore, it is inferred that the Holocene clays accumulated in the Changjiang Delta have similar composition on average to the present-day clay minerals in the Changjiang sediments. In Yang et al. (2001), geochemical data also indicate that the fine-grained sediments (<0.063 mm) of Core CM97 have similar composition to the modern fluvial sediments, diagnostic of their genetic inheritance.

Nevertheless, the four clay minerals in Core CM97 all show similar large variation in their percentages in the floodplain and fluvial facies (Units 3 and 4; Table 1; Fig. 2). The core sediments were deposited in various environments, from terrestrial (floodplain and fluvial facies), coastal (deltaic and estuarine facies) to shallow marine (neritic facies). Different hydrodynamic forces in these depositional environments may complicate the distribution of clay minerals, although they were all sourced from the Changjiang catchment. The clay mineral assemblages in the deltaic, neritic and estuarine facies (Units 1 and 2) are relatively stable and largely overlap with those from Core LGZ sediments. In comparison, the clays in the terrestrial floodplain and fluvial facies (Units 3 and 4) have different mineralogical characteristics especially in the relative amounts of illite and smectite (Fig. 4). Different hydrodynamic sorting and/or diagenesis in these variable depositional environments may account for this difference. In general, estuarine and neritic and part of deltaic environments are characterized by relatively deeper waters than those in floodplain and fluvial environments. The multi-sourced clayey sediments derived from the Changjiang catchment might have been well mixed in the marginal marine environments whereas the clays in the floodplain and river channel may better reflect their source characteristics due to rapid transport and deposition. Influence of hydrodynamic sorting on clay minerals in coastal and marine environments has been suggested by previous workers (Chamley, 1989; Dou et al., 2010; Gao et al., 2004; Steinke et al., 2008). In particular, smectite which has the smallest size of all clay minerals, is prone to winnowing by oceanic currents (Chamley, 1989). Nevertheless, the large fluctuation and extraordinary high content of smectite in floodplain and fluvial facies are primarily due to the changing provenances of clayey sediments in the late deglaciation (ca. 13–11 ka) rather than winnowing process during sediment transport and deposition. Sedimentary smectite is mostly derived from temperate–humid or from arid weathering processes, or from mafic and older sedimentary rocks (Chamley, 1989; Thiry, 2000). The Emeishan basalt in the upper Changjiang valley is regarded as the only large igneous province in China and one of the largest basalt provinces in the world (Xiao et al., 2003). The weathering of basalts may provide plenty of smectite for the upper Changjiang River, which has been evidenced from higher smectite contents in the upper Changjiang sediments (Mao et al., 2010; Wu et al., 2011). An et al. (2000) suggested that the Holocene climate optimum, as defined by peak summer monsoon precipitation, was asynchronous in central and eastern China, reaching a maximum at different times in different regions. In southwestern China the maximum

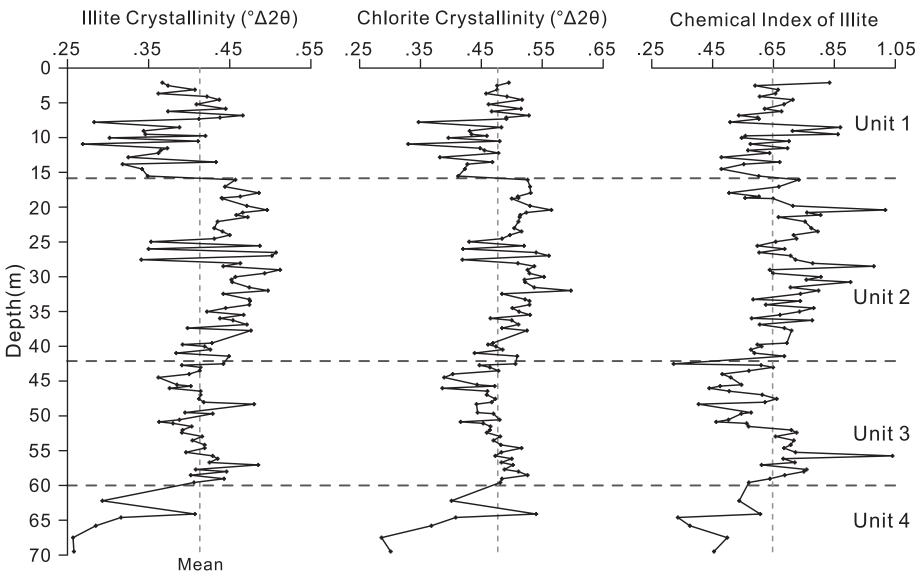

Fig. 3. Downcore variations of Illite crystallinity, chlorite crystallinity and chemical index of illite in Core CM97.

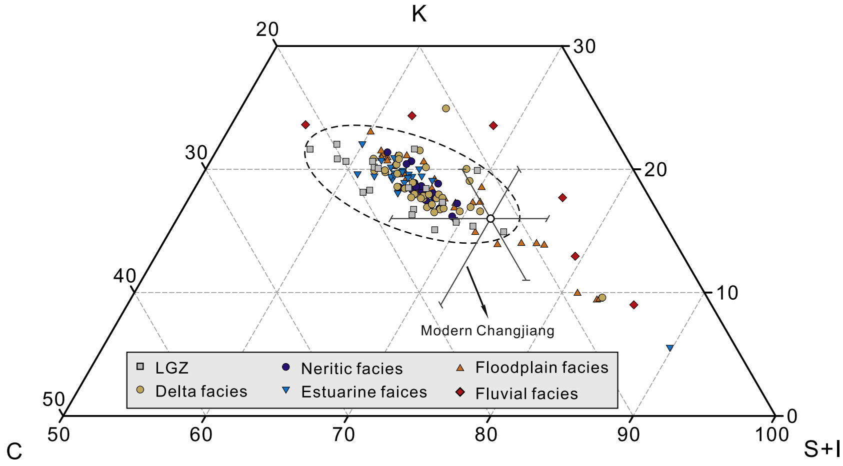

Fig. 4. Ternary diagram showing the comparison of clay mineral assemblages between the sediments from Core CM97 (shown as different depositional facies), Core LGZ (marked with dashed ellipse) and modern Changjiang River (Dou et al., 2010; Yang et al., 2003). K: kaolinite; C: chlorite; S: smectite; I: illite.

precipitation appeared ca. 11,000 years ago, which was probably related to the maximum landward extension of the Indian Summer Monsoon. Therefore, the intensified Indian Summer Monsoon during the late postglacial period to early Holocene (ca. 13–11 ka) might have brought a large amount of precipitation to the upper Changjiang valley, which promoted the weathering of Emeishan basalt and other basic rocks to smectite. This may explain the peak amounts of smectite in the floodplain and fluvial facies (Units 3 and 4) of Core CM97, while other samples in these two units have low smectite abundance, indicative of the complicated sediment source-to-sink transport pattern in the large Changjiang catchment.

5.2. Clay mineralogy indicating the monsoon evolution during the Holocene

Clay minerals in sediments can provide important constraints on continental weathering under different climate regimes (Biscaye, 1965; Chamley, 1989; Petschick et al., 1996; Singer, 1980, 1984; Thiry, 2000). Recent studies suggest that clay mineralogy in Asian marginal seas can indicate the evolution of EASM on orbital scale (Boulay et al., 2005; Liu et al., 2003, 2005; Wan et al., 2010), but primarily reflects sediment sources and hydrodynamic fractionation over shorter time scales such as the last glacial–interglacial interval (Dou et al., 2010; Steinke et al., 2008).

Schematically, illite and chlorite are interpreted to form in relatively very cold or hot-dry climate, while a hot and humid climate leads to stronger chemical weathering and the formation of kaolinite. Smectite minerals consist of several subgroups which may form in different chemical and climatic environments. Temperate climate tends to form incompletely altered minerals, mostly exfoliated illite and chlorite, irregular mixed-layers, vermiculite and degraded smectite, depending on the local climate. Sub-arid areas give way to well-crystallized Fe-smectite (Chamley, 1989; Singer, 1980, 1984). In fact, clay mineral assemblages in soils and sediments may not directly indicate chemical environments and paleoclimate but integrate records of different climatic impacts. Differentiation of clay assemblages during sediment transport and deposition, due to differential flocculation or size sorting, may significantly alter climate-induced signals, especially for the clays derived from large drainage basins and from multi sources. Therefore, crystallographic indices of clay minerals such as illite crystallinity (IC), chlorite crystallinity (ChC) and chemical index of illite (CII) are less influenced by sediment dynamic differentiation, and can better record climate signals than the absolute amounts (clay assemblages). These indices, as the characterization of mineral crystallinity degree, can reflect weathering conditions of sediment source area even if clay mineral contents are changed by hydrodynamic sorting during transport and deposition. In general, lower values of IC and ChC represent higher crystallinity, characteristic of weak hydrolysis in continental sources and dry and cold climate, while higher IC and ChC values indicates lower crystallinity, standing for strong hydrolysis caused by humid and warm climate (Chamley, 1989; Pandarinath, 2009; Pandarinath et al., 1999).

In the present day, the large Changjiang catchment covers different climate regimes with wide variation in temperature, precipitation and vegetation type. The upper part runs mainly through the Qinghai–Tibet Plateau and Yunnan–Guizhou Plateau, where the exposed rocks easily produce clays by strong physical erosion and limited chemical weathering under rigid climate. In contrast, the middle–lower basin is subject to subtropic climate with much higher annual precipitation and higher temperature on average than in the upper basin, which accounts for relatively strong chemical weathering and hydrolysis. Consequently, clay mineralogical indices of IC, ChC and CII yield lower values or higher crystallinity in the sediments of the upper Changjiang reaches, and higher values or poor crystallinity in the middle–lower reaches (Mao et al., 2010).

The crystallographic indices of IC, ChC and CII all exhibit similar and regular variations in Core CM97 (Fig. 3), showing higher values in Unit 2 (dominated by neritic and estuarine facies) and the lowest in Unit 4 (fluvial facies). Of particular note is the correspondence of the downcore variations of IC, ChC and CII with the well-known oxygen isotope curves of Dongge stalagmite in Guizhou Province, Southwest China (Dykoski et al., 2005; Wang et al., 2005) and of Sanbao Cave in Hubei Province, central South China (Dong et al., 2010) (Fig. 5). The oxygen isotopic records of these Chinese stalagmites are regarded as the best indication of Asian summer monsoon precipitation during the Holocene. Correspondingly, we infer that the indices of IC, ChC and CII in Core CM97 can also indicate the evolution of Holocene monsoon climate within the Changjiang catchment.

During the late deglaciation (about 13–11.5 ka, Units 3 and 4), the climate was colder and drier than at present; a weakened EASM (Dong et al., 2010; Dykoski et al., 2005) led to reduced precipitation in the Changjiang catchment. The sediments weathered in this climate have low IC, ChC and CII values (Fig. 5). The pollen data of Core CM97 also suggests cold and dry climate at ca. 13–11 ka (Yi et al., 2003b). The ratio of total organic carbon to total nitrogen (TOC/TN) exhibits extraordinary high values in Unit 4 (fluvial facies), suggesting the proximal input of terrestrial organic matter (Yang et al., 2011).

With the onset of Holocene, the enhanced EASM arrived at the maximum at about 9 ka and then gradually weakened towards the late

Table 1
Relative proportions of clay minerals in the <2 μm size fraction of the sediments from Cores LGZ and CM97 and crystallinity indices.

Cores	Depth (m)	Illite (%)	Kaolinite (%)	Chlorite (%)	Smectite (%)	IC (°Δ2θ)	ChC (°Δ2θ)	CII
LGZ	0.03	59.6	16.7	17.0	6.7	0.44	0.53	0.52
	0.12	65.1	15.1	16.4	3.4	0.48	0.59	0.54
	0.23	59.9	16.3	17.4	6.4	0.43	0.57	0.62
	0.31	62.9	18.4	15.3	3.3	0.41	0.54	0.52
	0.42	61.0	15.7	14.6	8.7	0.47	0.59	0.60
	0.52	60.8	17.3	14.7	7.2	0.43	0.53	0.70
	0.59	62.2	15.4	13.5	8.9	0.53	0.59	0.51
	0.69	68.7	14.9	11.6	4.8	0.44	0.52	0.42
	0.79	63.2	18.5	16.5	1.8	0.41	0.50	0.73
	0.89	54.5	21.6	21.8	2.0	0.40	0.55	0.74
	0.99	58.5	20.2	18.1	3.3	0.39	0.47	0.76
	1.19	66.9	19.9	11.0	2.2	0.34	0.40	0.47
	1.29	61.3	21.6	14.5	2.6	0.33	0.44	0.55
	1.39	58.1	20.1	17.8	4.0	0.43	0.53	0.58
	1.49	59.2	20.6	18.0	2.2	0.46	0.55	0.65
	1.59	58.6	18.1	19.9	3.4	0.43	0.48	0.68
	1.69	56.6	20.6	19.8	2.9	0.47	0.56	0.69
	1.79	57.7	18.3	19.3	4.7	0.47	0.56	0.60
	1.89	54.3	22.0	19.8	3.9	0.36	0.48	0.72
	1.97	56.1	20.8	20.3	2.7	0.44	0.53	0.81
CM97	2.11	64.7	16.6	13.9	4.9	0.37	0.50	0.83
	2.53	65.1	17.2	14.8	2.9	0.37	0.48	0.59
	3.13	61.3	16.9	16.0	5.7	0.41	0.48	0.66
	3.68	59.1	19.8	17.5	3.6	0.36	0.46	0.66
	4.10	62.4	17.1	15.5	5.0	0.42	0.49	0.60
	4.57	58.6	17.6	15.9	7.9	0.44	0.52	0.71
	5.23	59.3	17.8	15.8	7.1	0.41	0.46	0.68
	5.85	60.8	16.7	15.2	7.3	0.45	0.52	0.62
	6.23	58.0	19.6	16.7	5.6	0.37	0.47	0.68
	6.83	59.1	18.0	16.4	6.5	0.47	0.53	0.54
	7.12	61.7	17.6	15.0	5.7	0.44	0.49	0.60
	7.32	56.9	19.9	17.5	5.7	0.41	0.49	0.60
	7.78	61.8	20.0	11.7	6.5	0.28	0.35	0.51
	8.53	56.6	19.9	18.2	5.3	0.39	0.48	0.87
	9.05	51.5	18.0	14.7	15.9	0.34	0.43	0.71
	9.53	56.0	20.9	17.8	5.3	0.35	0.43	0.86
	9.75	63.7	17.6	16.1	2.6	0.42	0.46	0.56
	10.03	57.6	21.5	14.2	6.6	0.30	0.40	0.55
	10.53	59.7	20.4	16.4	3.5	0.41	0.48	0.70
	10.93	58.2	24.9	10.7	6.2	0.27	0.33	0.57
	11.53	60.2	21.1	15.9	2.8	0.37	0.45	0.70
	11.83	57.3	20.8	16.0	5.9	0.37	0.46	0.57
	12.23	28.2	9.6	7.4	54.9	0.36	0.48	0.64
	12.83	62.6	19.0	12.0	6.4	0.33	0.38	0.48
	13.53	60.6	17.7	16.7	5.0	0.43	0.47	0.67
	13.83	58.1	20.2	14.5	7.3	0.32	0.43	0.55
	14.53	57.1	16.6	12.4	13.9	0.34	0.42	0.48
	15.53	51.4	16.9	12.9	18.7	0.35	0.41	0.60
	16.07	54.9	18.6	17.3	9.3	0.46	0.53	0.73
	17.06	51.5	18.9	16.0	13.6	0.44	0.53	0.67
	17.95	59.5	16.5	15.7	8.3	0.49	0.53	0.50
	18.47	60.4	17.7	14.5	7.4	0.46	0.51	0.60
	18.67	61.5	18.0	15.4	5.2	0.44	0.51	0.56
	18.77	60.9	18.4	16.8	3.8	0.44	0.50	0.65
	19.81	58.4	16.8	14.9	9.9	0.47	0.53	0.71
	20.41	56.8	21.4	16.6	5.3	0.50	0.57	1.02
	20.78	61.3	16.8	15.1	6.8	0.47	0.52	0.76
	21.13	60.6	17.7	15.1	6.5	0.46	0.51	0.80
	21.43	58.6	17.2	13.7	10.5	0.47	0.51	0.67
	22.07	58.8	17.8	15.7	7.7	0.44	0.51	0.75
	23.03	58.3	18.3	15.7	7.7	0.43	0.50	0.77
	23.51	58.9	18.9	15.9	6.3	0.44	0.52	0.80
	24.01	61.0	18.6	15.5	4.8	0.45	0.50	0.72
	24.53	60.4	18.1	15.0	6.5	0.43	0.48	0.73
	24.97	59.7	18.8	14.3	7.2	0.35	0.43	0.66
	25.56	66.7	16.2	14.6	2.5	0.49	0.52	0.60
	26.00	61.2	20.6	15.2	2.9	0.35	0.42	0.69
	26.52	61.0	17.1	15.6	6.3	0.51	0.54	0.60
	26.99	58.3	18.3	16.3	7.0	0.50	0.56	0.71
	27.55	59.8	20.4	15.7	4.1	0.34	0.42	0.72
	28.07	59.0	18.6	15.9	6.4	0.46	0.51	0.78
	28.50	60.9	18.5	17.2	3.4	0.44	0.54	0.98
	29.00	61.3	16.8	15.2	6.7	0.51	0.53	0.64
CM97	29.51	61.1	17.5	15.8	5.6	0.49	0.53	0.65
	30.02	57.6	19.6	19.5	3.2	0.46	0.55	0.81
	30.43	59.3	18.5	16.9	5.3	0.45	0.52	0.76
	30.77	57.5	19.5	18.4	4.6	0.45	0.52	0.90
	31.53	49.3	15.9	14.6	20.2	0.47	0.54	0.71
	32.00	56.1	19.2	17.3	7.4	0.50	0.60	0.80
	32.45	60.0	18.0	16.2	5.7	0.44	0.48	0.74
	33.25	59.7	19.6	15.9	4.8	0.47	0.52	0.58
	33.50	58.1	21.0	16.3	4.6	0.48	0.53	0.74
	34.02	55.0	18.3	15.5	11.2	0.47	0.53	0.62
	34.51	58.4	20.7	17.3	3.6	0.45	0.50	0.78
	35.02	57.4	19.4	17.3	5.9	0.42	0.51	0.74
	35.48	60.3	17.4	15.5	6.8	0.47	0.53	0.67
	35.97	60.0	19.9	16.2	3.9	0.44	0.47	0.58
	36.26	58.5	19.7	16.9	4.9	0.45	0.50	0.78
	36.87	60.2	19.5	15.1	5.3	0.47	0.51	0.60
	37.38	55.2	22.1	18.0	4.8	0.40	0.48	0.69
	37.73	59.9	20.2	16.9	3.0	0.48	0.53	0.71
	39.54	56.8	19.4	15.8	7.9	0.43	0.47	0.69
	39.75	60.1	20.0	15.0	4.9	0.39	0.46	0.60
	40.02	60.2	18.9	16.6	4.3	0.42	0.47	0.61
	40.48	57.9	19.5	17.0	5.6	0.43	0.49	0.58
	40.98	61.0	19.1	14.5	5.3	0.38	0.44	0.59
	41.43	58.3	18.1	17.5	6.1	0.45	0.51	0.69
	42.52	19.8	5.6	4.6	70.0	0.44	0.51	0.32
	42.73	61.2	19.3	16.1	3.3	0.39	0.45	0.61
	43.02	59.6	19.8	16.3	4.3	0.41	0.46	0.65
	43.52	46.1	14.0	10.9	29.0	0.41	0.48	0.57
	44.00	68.0	18.5	11.4	2.1	0.40	0.40	0.48
	44.48	59.5	20.6	14.4	5.5	0.36	0.39	0.51
	45.52	47.3	14.0	9.8	28.9	0.39	0.44	0.54
	45.73	32.8	9.4	7.8	49.9	0.40	0.47	0.47
	46.02	67.5	17.3	12.1	3.1	0.38	0.39	0.44
	46.45	59.6	19.2	14.3	6.9	0.41	0.46	0.50
	46.97	59.5	19.6	16.1	4.8	0.41	0.46	0.61
	47.56	58.5	19.2	16.3	5.9	0.41	0.47	0.66
	48.03	59.3	21.1	15.3	4.3	0.42	0.47	0.62
	48.32	67.2	14.9	13.6	4.3	0.48	0.44	0.40
	49.53	52.5	17.3	13.8	16.4	0.40	0.44	0.58
	49.70	50.9	16.9	14.1	18.2	0.43	0.47	0.54
	50.56	27.7	9.5	7.6	55.2	0.39	0.48	0.50
	50.86	57.0	17.6	14.4	11.0	0.36	0.42	0.46
	51.08	38.0	13.8	9.3	38.8	0.38	0.45	0.56
	51.52	56.2	17.3	12.6	13.9	0.40	0.47	0.57
	52.03	55.9	21.2	17.0	6.0	0.39	0.46	0.71
	52.42	57.3	21.1	16.1	5.5	0.39	0.46	0.73
	52.97	57.3	18.1	16.1	8.5	0.42	0.48	0.66
	53.53	56.7	20.2	16.7	6.4	0.40	0.47	0.72
	54.16	57.1	20.9	16.8	5.2	0.42	0.48	0.71
	54.63	48.5	18.4	14.9	18.1	0.42	0.52	0.68
	55.23	56.3	20.9	17.2	5.6	0.40	0.48	0.72
	55.75	56.8	23.0	16.9	3.2	0.43	0.47	1.04
	56.17	58.2	18.5	17.2	6.1	0.44	0.50	0.68
	56.70	56.2	20.3	16.6	6.9	0.43	0.48	0.72
	57.05	59.4	18.7	16.1	5.8	0.49	0.50	0.61
	57.71	55.2	21.5	16.9	6.3	0.41	0.49	0.76
	58.01	55.3	20.7	16.9	7.2	0.45	0.51	0.75
	58.52	47.2	13.9	12.6	26.3	0.40	0.53	0.69
	59.04	57.3	19.6	16.6	6.5	0.44	0.48	0.64
	59.58	28.4	9.9	8.9	52.7	0.41	0.48	0.57
	62.20	50.8	24.3	13.3	11.5	0.29	0.40	0.54
	64.10	44.1	23.6	21.2	11.1	0.41	0.54	0.61
	64.60	26.1	9.0	5.4	59.5	0.32	0.41	0.34
	65.80	32.9	12.9	7.6	46.6	0.29	0.37	0.38
	67.50	51.4	17.7	6.1	24.8	0.26	0.29	0.50
	69.50	50.2	23.5	8.0	18.2	0.26	0.30	0.45

Note: IC = Illite Crystallinity; ChC = Chlorite Crystallinity; CII = Chemical Index of Illite.

Holocene (An et al., 2000; Dong et al., 2010; Dykoski et al., 2005; Wang et al., 2005). The strengthening EASM climate might have caused abundant rainfall and enhanced chemical weathering in the Changjiang catchment, especially in the middle–lower basins, which consequently resulted in a significant supply of poorly-crystallized clay minerals

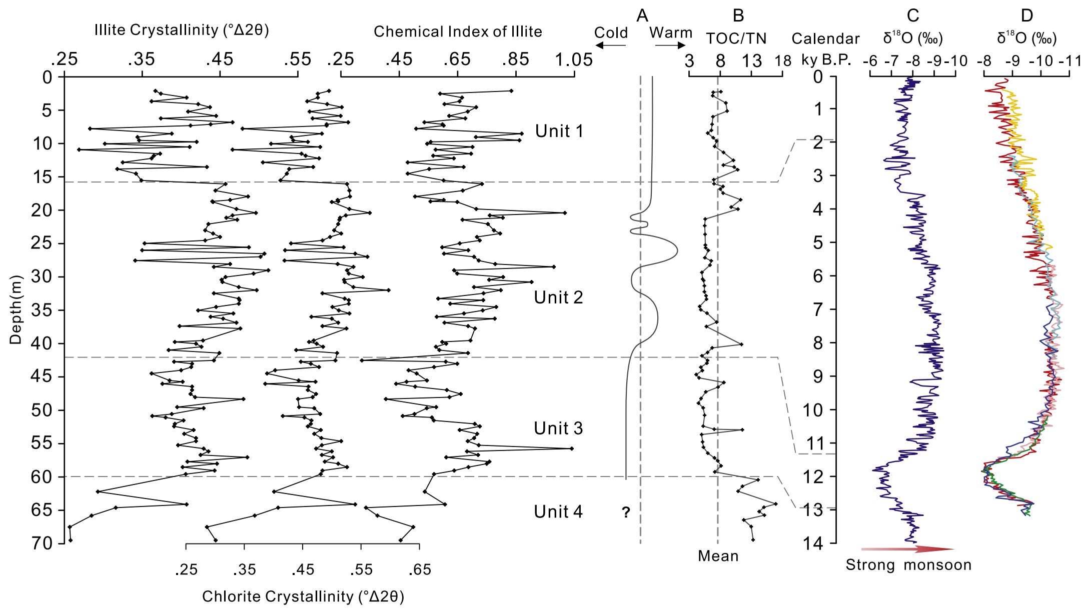

Fig. 5. Comparison of Illite crystallinity, chlorite crystallinity and chemical index of illite of Core CM97 sediments with the other proxies indicating climate change during the Holocene. A): Pollen records of Core CM97 (Yi et al., 2003b); B): Ratio of Total organic carbon to total nitrogen (TOC/TN) (Yang et al., 2011); C): Oxygen isotopic ratios of Dongge Stalagmite in Guizhou Province, Southwest China (Dykoski et al., 2005); D): Oxygen isotopic curves from Sanbao Cave in Hubei Province, central South China (Dong et al., 2010).

with high IC, ChC and CII values into the Changjiang river mouth (Unit 2, Fig. 5). Pollen and organic geochemical data further imply that the paleoclimate was warm and humid at ca. 9–4 ka (Yi et al., 2003b), and marine organic matter dominated the estuarine to shallow marine depositional environments (Yang et al., 2011).

Over the past 1500 to 2000 years, the EASM was weaker than in the early-mid Holocene, and the Changjiang Delta rapidly prograded with the transition from shallow marine to deltaic sedimentary environment (Hori et al., 2001a,b, 2002a,b; Li et al., 2000; Yang et al., 2011). The deltaic sediments (Unit 1) have lower IC, ChC and CII values relative to the shallow marine and estuarine sediments (Unit 2) (Fig. 5), also suggesting weaker chemical weathering with the decrease of monsoon precipitation during the late Holocene. Another possibility regarding the origin of clays in Unit 1 is that increasing anthropogenic activity over the last 2000 years caused strong erosion in the Changjiang catchment, especially in the upper basin (Saito et al., 2001), which resulted in the dominance of the upper Changjiang-derived sediments in the deltaic deposition since 2 ka. The clay minerals derived from the upper Changjiang reaches generally have low IC, ChC and CII values because of weak chemical weathering under an unfavorable climate regime. The crystallographic indices including IC, ChC and CII of clay minerals from the Holocene sediments in the Changjiang Delta appear to closely reflect changes in the paleoclimate across the large drainage basin, although the resolution of change is less precise than that obtained from the well-known stalagmite records.

6. Conclusions

The clay mineral compositions of two cores from the Changjiang Delta were investigated in order to examine the origins of the clays deposited in the Changjiang estuary and delta, and to evaluate the impact of monsoon climate on the weathering, transport and deposition of clays in the catchment during the Holocene. The major clay mineral assemblages of the Holocene sediments are overall similar to the clays of the modern Changjiang, dominated by illite, but exhibit large fluctuations in terrestrial depositional environment (fluvial to floodplain facies) in the early Holocene. The estuarine, shallow marine and deltaic environments are characterized by relatively stable clay mineralogy. Independent of the absolute abundance of clay minerals, the crystallographic indices of illite crystallinity, chlorite crystallinity and chemical index of illite, show regular variations in Core CM97 that were used to identify four depositional units with unique clay mineral patterns.

The crystallographic indices of illite and chlorite in sediments as the indication of clay mineral crystallinity, are closely related to the continent weathering and climatic environments. The variations of these indices in the Holocene sediments in the Changjiang Delta are closely comparable with the well-known oxygen isotopic curves of cave carbonates in southeast China. The results suggest that the crystallographic indices of specific clay minerals can distinctly indicate monsoon climate variability in the large drainage basin. Pollen and organic data of the core sediments further indicate similar paleoclimatic changes in the catchment and delta during the Holocene. In particular, weakening in late deglaciation (ca. 13–11.5 ka) and strengthening in the early-mid Holocene (ca. 11.5–4 ka) of EASM would be expected to have resulted in a large variability in precipitation and temperature over the vast catchment, with a consequent change in the intensity of chemical weathering, as evidenced by the fluctuation of crystallographic indices of the clay minerals.

The clay mineral assemblages are primarily determined by the various sources of clays in the Changjiang catchment and transport and depositional processes, and thus, cannot distinctly reflect EASM evolution in the Holocene. Smectite, for example, has the largest variation in content from 13,000–11,300 cal years B.P., probably reflecting the significant contribution of clays from the upper Changjiang valley with the enhancing Indian Summer Monsoon at that time.

Acknowledgments

This work was supported by the National Natural Science Foundation of China (grant no. 41076018). We thank Yoshiki Saito, Yanguang Dou, Xisheng Fang and Hongbo Zheng for their help during the sampling and analytic work. We are grateful to John Keeling and two anonymous reviewers for their constructive comments on the manuscript.

References

Alley, R.B., Ágústsdóttir, A.M., 2005. The 8 k event: cause and consequences of a major Holocene abrupt climate change. Quaternary Science Reviews 24, 1123–1149.

An, Z., Porter, S.C., Kutzbach, J.E., Xiao, W., Wang, S.M., Liu, X.D., Li, X.Q., Zhou, W.J., 2000. Asynchronous Holocene optimum of the East Asian monsoon. Quaternary Science Reviews 19, 743–762.

Árkai, P., Ghabrial, D.S., 1997. Chlorite crystallinity as an indicator of metamorphic grade of low-temperature meta-igneous rocks; a case study from the Bukk Mountains, Northeast Hungary. Clay Minerals 32, 205–222.

Árkai, P., Sassi, F.P., Sassi, R., 1995. Simultaneous measurements of chlorite and illite crystallinity; a more reliable tool for monitoring low- to very low grade metamorphisms in metapelites; a case study from the Southern Alps (NE Italy). European Journal of Mineralogy 7, 1115–1128.

Atahan, P., Itzstein-Davey, F., Taylor, D., Dodson, J., Qin, J.G., Zheng, H.B., Brooks, A., 2008. Holocene-aged sedimentary records of environmental changes and early agriculture in the lower Yangtze, China. Quaternary Science Reviews 27, 556–570.

Biscaye, P., 1965. Mineralogy and sedimentation of Recent deep-sea clay in the Atlantic Ocean and adjacent seas and oceans. Geological Society of America Bulletin 76, 803–832.

Bond, G., Kromer, B., Beer, J., Muscheler, R., Evans, M.N., Showers, W., Hoffmann, S., Lotti-Bond, R., Hajdas, I., Bonani, G., 2001. Persistent solar influence on North Atlantic climate during the Holocene. Science 294, 2130–2136.

Boulay, S., Colin, C., Trentesaux, A., Frank, N., Liu, Z.F., 2005. Sediment sources and East Asian monsoon intensity over the last 450 ky. Mineralogical and geochemical investigations on South China Sea sediments. Palaeogeography, Palaeoclimatology, Palaeoecology 228, 260–277.

Chamley, H., 1989. Clay sedimentology. Springer, Berlin.

Chen, J., Wan, G., Zhang, D.D., Chen, Z., Xu, J., Xiao, T., Huang, R., 2005a. The 'Little Ice Age' recorded by sediment chemistry in Lake Erhai, southwest China. The Holocene 15, 925–931.

Chen, Z.Y., Wang, Z.H., Schneiderman, J., Tao, J., Cai, Y., 2005b. Holocene climate fluctuations in the Yangtze delta of eastern China and the Neolithic response. The Holocene 15, 915–924.

Chen, F., Yu, Z., Yang, M., Ito, E., Wang, S., Madsen, D.B., Huang, X., Zhao, Y., Sato, T., John B. Birks, H., Boomer, I., Chen, J., An, C., Wünnemann, B., 2008. Holocene moisture evolution in arid central Asia and its out-of-phase relationship with Asian monsoon history. Quaternary Science Reviews 27, 351–364.

Chen, W., Wang, W.M., Dai, X.R., 2009. Holocene vegetation history with implications of human impact in the Lake Chaohu area, Anhui Province, East China. Vegetation History and Archaeobotany 18, 137–146.

China Ministry of Water Resources, 2011. Sediment Bulletin of Chinese Rivers. China Water Resources and Hydropower Press . p. 70.

Chu, K.C., 1973. A preliminary study on the climatic fluctuations during the last 5,000 years in China. Scicntia Sinica 16, 226–256.

deMenocal, P., Ortiz, J., Guilderson, T., Sarnthein, M., 2000. Coherent high- and low-latitude climate variability during the Holocene warm period. Science 288, 2198–2202.

Denton, G.H., Karlén, W., 1973. Holocene climatic variations—their pattern and possible cause. Quaternary Research 3, 155–205.

Dong, J., Wang, Y., Cheng, H., Hardt, B., Edwards, R.L., Kong, X., Wu, J., Chen, S., Liu, D., Jiang, X., Zhao, K., 2010. A high-resolution stalagmite record of the Holocene East Asian monsoon from Mt. Shennongjia, central China. The Holocene 20, 257–264.

Dou, Y.G., Yang, S.Y., Liu, Z.X., Clift, P.D., Yu, H., Berne, S., Shi, X.F., 2010. Clay mineral evolution in the central Okinawa Trough since 28 ka: implications for sediment provenance and paleoenvironmental change. Palaeogeography, Palaeoclimatology, Palaeoecology 288, 108–117.

Dykoski, C.A., Edwards, R.L., Cheng, H., Yuan, D., Cai, Y., Zhang, M., Lin, Y., Qing, J., An, Z., Revenaugh, J., 2005. A high-resolution, absolute-dated Holocene and deglacial Asian monsoon record from Dongge Cave, China. Earth and Planetary Science Letters 233, 71–86.

Fan, D.J., Yang, Z.S., Mao, D., Guo, Z.G., 2001. Clay minerals and geochemistry of the sediments from the Yangtze and Yellow Rivers. Marine Geology and Quaternary Geology 21, 7–12 (in Chinese with English abstract).

Fang, X.S., Shi, X.F., Wang, G.Q., 2007. Distributions of clay minerals in surface sediements from the Changjiang River subaqueous delta and their affecting factors. Advances in Marine Science 25, 419–427 (in Chinese with English abstract).

Fleitmann, D., Burns, S.J., Mangini, A., Mudelsee, M., Kramers, J., Villa, I., Neff, U., Al-Subbary, A.A., Buettner, A., Hippler, D., Matter, A., 2007. Holocene ITCZ and Indian monsoon dynamics recorded in stalagmites from Oman and Yemen (Socotra). Quaternary Science Reviews 26, 170–188.

Gao, S., Zhou, X.J., Jia, J.J., 2004. Clay mineral suites of the coastal mud belt associated with the Changjiang River. Asociación Argentina de Sedimentología Revista 11, 1–8.

Hodell, D.A., Cuitis, J.H., Jones, G.A., Higuera-Gundy, A., Brenner, M., Binfordll, M.W., Dorsey, K.T., 1991. Reconstruction of Caribbean climate change over the past 10,500 years. Nature 352, 790–793.

Hong, Y.T., Hong, B., Lin, Q.H., Shibata, Y., Hirota, M., Zhu, Y.X., Leng, X.T., Wang, Y., Wang, H., Yi, L., 2005. Inverse phase oscillations between the East Asian and Indian Ocean summer monsoons during the last 12 000 years and paleo-El Niño. Earth and Planetary Science Letters 231, 337–346.

Hori, K., Saito, Y., Zhao, Q.H., Cheng, X.R., Wang, P.X., Sato, Y., Li, C.X., 2001a. Sedimentary facies and Holocene progradation rates of the Changjiang (Yangtze) delta, China. Geomorphology 41, 233–248.

Hori, K., Saito, Y., Zhao, Q.H., Cheng, X.R., Wang, P.X., Sato, Y., Li, C.X., 2001b. Sedimentary facies of the tide-dominated paleo-Changjiang (Yangtze) estuary during the last transgression. Marine Geology 177, 331–351.

Hori, K., Saito, Y., Zhao, Q.H., Wang, P.X., 2002a. Architecture and evolution of the tide-dominated Changjiang (Yangtze) River delta, China. Sedimentary Geology 146, 249–264.

Hori, K.H., Saito, Y.S., Zhao, Q.Z., Wang, P.W., 2002b. Control of incised-valley fill stacking patterns by accelerated and decelerated sea-level rise: the Changjiang example during the last deglaciation. Geo-Marine Letters 22, 127–132.

Ji, J., Browne, P.R.L., 2000. Relationship between illite crystallinity and temperature in active geothermal systems of New Zealand. Clays and Clay Minerals 48, 139–144.

Kleinen, T., Tarasov, P., Brovkin, V., Andreev, A., Stebich, M., 2011. Comparison of modeled and reconstructed changes in forest cover through the past 8000 years: Eurasian perspective. The Holocene 21, 723–734.

Li, C.X., Chen, Q.Q., Zhang, J.Q., Yang, S.Y., Fan, D.D., 2000. Stratigraphy and paleoenvironmental changes in the Yangtze Delta during the Late Quaternary. Journal of Asian Earth Sciences 18, 453–469.

Li, Z.F., Zhang, Y.L., Li, Y., Zhao, J., 2010. Palynological records of Holocene monsoon change from the Gulf of Tonkin (Beibuwan), northwestern South China Sea. Quaternary Research 74, 8–14.

Liu, K.B., Sun, S., Jiang, X., 1992. Environmental change in the Yangtze River delta since 12,000 years B.P. Quaternary Research 38, 32–45.

Liu, K.B., Yao, Z., Thompson, L.G., 1998. A pollen record of Holocene climatic changes from the Dunde ice cap, Qinghai–Tibetan Plateau. Geology 26, 135–138.

Liu, Z.F., Trentesaux, A., Clemens, S.C., Colin, C., Wang, P.X., Huang, B., Boulay, S., 2003. Clay mineral assemblages in the northern South China Sea: implications for East Asian monsoon evolution over the past 2 million years. Marine Geology 201, 133–146.

Liu, Z.F., Colin, C., Trentesaux, A., Siani, G., Frank, N., Blamart, D., Farid, S., 2005. Late Quaternary climatic control on erosion and weathering in the eastern Tibetan Plateau and the Mekong Basin. Quaternary Research 63, 316–328.

Mao, C.P., Chen, J., Yuan, X.F., Yang, Z., Balsam, W., Ji, J.F., 2010. Seasonal variation in the mineralogy of the suspended particulate matter of the lower Changjiang River at Nanjing, China. Clays and Clay Minerals 58, 691–706.

Mas, A., Guisseau, D., Patrier Mas, P., Beaufort, D., Genter, A., Sanjuan, B., Girard, J.P., 2006. Clay minerals related to the hydrothermal activity of the Bouillante geothermal field (Guadeloupe). Journal of Volcanology and Geothermal Research 158, 380–400.

Mayewski, P.A., Rohling, E.E., Curt Stager, J., Karlén, W., Maasch, K.A., David Meeker, L., Meyerson, E.A., Gasse, F., van Kreveld, S., Holmgren, K., Lee-Thorp, J., Rosqvist, G., Rack, F., Staubwasser, M., Schneider, R.R., Steig, E.J., 2004. Holocene climate variability. Quaternary Research 62, 243–255.

Pandarinath, K., 2009. Clay minerals in SW Indian continental shelf sediment cores as indicators of provenance and palaeomonsoonal conditions: a statistical approach. International Geology Review 51, 145–165.

Pandarinath, K., Prasad, S., Gupta, S.K., 1999. A 75 Ka record of palaeoclimatic changes inferred from crystallinity of illite from Nal Sarovar, Western India. Journal Geological Society of India 54, 512–522.

Petschick, R., Kuhn, G., Gingele, F., 1996. Clay mineral distribution in surface sediments of the South Atlantic: sources, transport, and relation to oceanography. Marine Geology 130, 203–229.

Saito, Y., Yang, Z., Hori, K., 2001. The Huanghe (Yellow River) and Changjiang (Yangtze River) deltas: a review on their characteristics, evolution and sediment discharge during the Holocene. Geomorphology 41, 219–231.

Shen, J., Jones, R.T., Yang, X., Dearing, J.A., Wang, S., 2006. The Holocene vegetation history of Lake Erhai, Yunnan province southwestern China: the role of climate and human forcings. The Holocene 16, 265–276.

Shi, Y., Kong, Z., Wang, S., Tang, L., Wang, F., Yao, T., Zhao, X., Zhang, P., Shi, S., 1993. Mid-holocene climates and environments in China. Global and Planetary Change 7, 219–233.

Shi, Y., Yao, T., Yang, B., 1999. Decadal climatic variations recorded in Guliya ice core and comparison with the historical documentary data from East China during the last 2000 years. Science in China Series D: Earth Sciences 42, 91–100.

Singer, A., 1980. The paleoclimatic interpretation of clay minerals in soils and weathering profiles. Earth-Science Reviews 15, 303–326.

Singer, A., 1984. The paleoclimatic interpretation of clay minerals in sediments—a review. Earth-Science Reviews 21, 251–293.

Steinke, S., Hanebuth, T.J.J., Vogt, C., Stattegger, K., 2008. Sea level induced variations in clay mineral composition in the southwestern South China Sea over the past 17,000 yr. Marine Geology 250, 199–210.

Thiry, M., 2000. Palaeoclimatic interpretation of clay minerals in marine deposits: an outlook from the continental origin. Earth-Science Reviews 49, 201–221.

Thompson, L.G., Yao, T., Davis, M.E., Mosley-Thompson, E., Mashiotta, T.A., Lin, P.-N., Mikhalenko, V.N., Zagorodnov, V.S., 2006. Holocene climate variability archived in the Puruogangri ice cap on the central Tibetan Plateau. Annals of Glaciology 43, 61–69.

Wan, S., Li, A., Clift, P.D., Wu, S., Xu, K., Li, T., 2010. Increased contribution of terrigenous supply from Taiwan to the northern South China Sea since 3 Ma. Marine Geology 278, 115–121.

Wang, Y., Cheng, H., Edwards, R.L., He, Y., Kong, X., An, Z., Wu, J., Kelly, M.J., Dykoski, C.A., Li, X., 2005. The Holocene Asian monsoon: links to solar changes and North Atlantic climate. Science 308, 854–857.

Wu, W., Xu, S., Lu, H., Yang, J., Yin, H., Liu, W., 2011. Mineralogy, major and trace element geochemistry of riverbed sediments in the headwaters of the Yangtze, Tongtian River and Jinsha River. Journal of Asian Earth Sciences 40, 611–621.

Xiao, L., Xu, Y., He, B., 2003. Emei mantle plume–subcontinental lithosphere interaction: Sr–Nd and O isotopic evidences from low-Ti and high-Ti basalts. Geological Journal of China Universities 9, 207–225 (in Chinese with English abstract).

Xiao, J., Wu, J., Si, B., Liang, W., Nakamura, T., Liu, B., Inouchi, Y., 2006. Holocene climate changes in the monsoon/arid transition reflected by carbon concentration in Daihai Lake of Inner Mongolia. The Holocene 16, 551–560.

Yang, Z.S., 1988. Clay mineral assemblages and chemical characters in Changjiang, Huanghe and Zhujiang sediments, and its relation with the climate environment in the source areas. Oceanologia Et Limnologia Sinica 19, 336–346.

Yang, S.Y., Li, C.X., Zhao, Q.H., Yoshiki, S., Kazuaki, H., 2001. Element geochemistry of Holocene sediment and paleoenvironmental change in the Changjiang Estuary. Science in China Series B: Chemistry 44, 40–46.

Yang, S.Y., Jung, H.S., Lim, D.I., Li, C.X., 2003. A review on the provenance discrimination of sediments in the Yellow Sea. Earth-Science Reviews 63, 93–120.

Yang, S.Y., Tang, M., Yim, W.W.-S., Zong, Y.Q., Huang, G.Q., Switzer, A.D., Saito, Y., 2011. Burial of organic carbon in Holocene sediments of the Zhujiang (Pearl River) and Changjiang (Yangtze River) estuaries. Marine Chemistry 123, 1–10.

Yasuda, Y., Fujiki, T., Nasu, H., Kato, M., Morita, Y., Mori, Y., Kanehara, M., Toyama, S., Yano, A., Okuno, M., He, J., Ishihara, S., Kitagawa, H., Fukusawa, H., Naruse, T., 2004. Environmental archaeology at the Chengtoushan site, Hunan Province, China, and implications for environmental change and the rise and fall of the Yangtze River civilization. Quaternary International 123, 149–158.

Yi, S., Saito, Y., 2004. Latest pleistocene climate variation of the East Asian monsoon from pollen records of two East China regions. Quaternary International 121, 75–87.

Yi, S., Saito, Y., Oshima, H., Zhou, Y., Wei, H., 2003a. Holocene environmental history inferred from pollen assemblages in the Huanghe (Yellow River) delta, China: climatic change and human impact. Quaternary Science Reviews 22, 609–628.

Yi, S., Saito, Y., Zhao, Q.H., Wang, P.X., 2003b. Vegetation and climate changes in the Changjiang (Yangtze River) Delta, China, during the past 13,000 years inferred from pollen records. Quaternary Science Reviews 22, 1501–1519.

Yi, S., Saito, Y., Yang, D.Y., 2006. Palynological evidence for Holocene environmental change in the Changjiang (Yangtze River) Delta, China. Palaeogeography, Palaeoclimatology, Palaeoecology 241, 103–117.

Zhan, W., Yang, S., Liu, X., Li, J., Choi, M., 2010. Reconstruction of flood events over the last 150 years in the lower reaches of the Changjiang River. Chinese Science Bulletin 55, 2268–2274.

Zhang, D.E., 2006. Environmental change and agricultural development in historical documentary records for Northwest China. Advances in Climate Change Research 2, 1673–1719.

Zhang, J., Jia, Y., Lai, Z., Long, H., Yang, L., 2011. Holocene evolution of Huangqihai Lake in semi-arid northern China based on sedimentology and luminescence dating. The Holocene 21, 1261–1268.

Zong, Y.Q., Lloyd, J.M., Leng, M.J., Yim, W.W.-S., Huang, G.Q., 2006. Reconstruction of Holocene monsoon history from the Pearl River Estuary, southern China, using diatoms and carbon isotope ratios. The Holocene 16, 251–263.